Available online at www.sciencedirect.com
ScienceDirect
Trans. Nonferrous Met. Soc. China 23(2013) 1245−1252

Transactions of Nonferrous Metals Society of China
www.tnmsc.cn

Effect of ultrasonic vibration on Fe-containing intermetallic compounds of hypereutectic Al−Si alloys with high Fe content

Chong LIN, Shu-sen WU, Gu ZHONG, Li WAN, Ping AN

State Key Laboratory of Materials Processing and Die & Mould Technology,
Huazhong University of Science and Technology, Wuhan 430074, China

Received 13 February 2012; accepted 23 May 2012

Abstract: The Fe-containing intermetallic compounds with high melting point in hypereutectic Al−Si alloys can improve the heat resistance and wear resistance at elevated temperatures. However, the long needle-like Fe-containing compounds in the alloys produced by conventional casting process are detrimental to the strength of matrix. The effect of ultrasonic vibration (USV) on the morphology change of Fe-containing intermetallic compounds in the hypereutectic Al−17Si−*x*Fe (*x*=2, 3, 4, 5) alloys was systematically studied. The results show that, the Fe-containing intermetallic compounds are mainly composed of long needle-like β-Al_5FeSi phase with a small amount of plate-like δ-Al_4FeSi_2 phase in Al−17Si−2Fe alloy produced by conventional casting process. With the increase of Fe content from 2% to 5% in the alloys, the amount of plate-like or coarse needle-like δ-Al_4FeSi_2 phase increases while the amount of long needle-like β-Al_5FeSi phases decreases. In Al−17Si−5Fe alloy, the Fe-containing intermetallic compounds exist mainly as coarse needle-like δ-Al_4FeSi_2 phase. After USV treatment, the Fe-containing compounds in the Al−17Si−*x*Fe alloys are refined and exist mainly as δ-Al_4FeSi_2 particles, with average grain size ranging from 26 μm to 37 μm, and only a small amount of β-Al_5FeSi phases remain. The mechanism of USV on the morphology of Fe-containing intermetallic compounds was also discussed.

Key words: hypereutectic Al−Si alloy; ultrasonic vibration; Fe-containing intermetallic compound

1 Introduction

Hypereutectic Al−Si alloys are important materials for automotive applications such as engine blocks and pistons, because of their relatively high temperature resistance, low thermal expansion coefficient and high wear resistance [1,2]. Iron is usually considered to be an impurity element in aluminum casting alloys where its content is under limitation [3,4]. The coarse needle-like or plate-like Fe-containing intermetallic compounds such as β-Al_5FeSi and δ-Al_4FeSi_2 phases, which are very hard and brittle and act as potential sites for crack initiation, are detrimental to the mechanical properties. In addition, coarse Fe-containing needles or platelets impede the flow of interdendritic liquid during feeding, and thus shrinkage pore forms more easily [5]. Nevertheless, investigations showed that δ-Al_4FeSi_2 and β-Al_5FeSi phases are relatively stable at temperature up to 300 °C [6]. Therefore, the Fe-containing intermetallic compounds with high melting point formed in hypereutectic Al−Si alloys can improve the mechanical properties at elevated temperatures. The morphology of the Fe-containing intermetallic compounds plays the most important role in determining the mechanical properties of the alloys. Recently, researches have been focused on changing the morphology of the Fe-containing intermetallic compounds.

It has been proved that the morphology of Fe-containing intermetallic compounds can be modified by neutralizing elements addition (such as Mn, Cr) [7], melt superheating [8] and rapid solidification process [9]. However, the increase of the total Fe and Mn concentration above 2.0%−2.5% may result in the formation of primary $Al_{15}(Fe,Mn)_3Si_2$ particles. The particles are of polygonal shape and often exist as big clusters. They are evidently harmful to many properties, in particular, ductility and machinability [10]. Therefore, the neutralization effect of Mn on the morphology of Fe-intermetallic compounds is limited in hypereutectic

Foundation item: Project (2012CB619600) supported by the National Basic Research Program of China; Project (50775086) supported by the National Natural Science Foundation of China
Corresponding author: Shu-sen WU; Tel: +86-27-87556262; E-mail: ssw636@hust.edu.cn
DOI: 10.1016/S1003-6326(13)62589-3

Al−Si alloys with high Fe content. Applications of melt superheating and rapid solidification process are also limited because of costly equipment and complicated process.

The treatment of molten aluminum and its alloys using ultrasonic vibration (USV) is a relatively new and environmentally safe technology with uncomplicated process and low cost. It has been reported that USV can effectively modify the α(Al) and primary Si in hypoeutectic and hypereutectic Al−Si alloys respectively [11−13]. OSAWA et al [14] studied the effect of USV on the morphological changes of Fe-containing intermetallic compounds of the Al−xSi−4Fe (x=6, 12, 18, mass fraction) alloys, and the results showed that the Fe-containing intermetallic compounds are refined after USV treatment, with the average equivalent diameter ranging from 59 μm to 77 μm. KHALIFA et al [15] studied the effect of USV on the Fe-intermetallic phases in ADC12 die cast alloy with 0.78% Fe, and the results showed that USV can effectively convert the long plate-like β phase to a highly compacted fine polyhedral/globular form in this alloy with low iron content. However, the influence of USV treatment on the Fe-containing intermetallic compounds in hypereutectic Al−Si alloys with different Fe contents has not been systematically investigated. It is not clear whether the β phase changes with the increase of Fe content, and whether the solidification mechanism changes after the USV treatment.

The aim of the present work is to systematically investigate the effect of USV treatment on the morphology and size of Fe-containing intermetallic compounds of Al−17Si−xFe (x=2, 3, 4, 5, mass fraction) alloys. In addition, the mechanism of USV on the morphology of Fe-containing intermetallic compounds is also discussed.

2 Experimental

The installation of USV in Ref. [13] was employed in this experiment. The applied ultrasonic power was 1.2 kW and the frequency of USV was 20 kHz. The ultrasonic vibrator consists of transducer and amplitude transforming rod made with titanium alloy.

The Al−17Si−xFe (x=2, 3, 4, 5) alloys were prepared with raw materials of Al−25.8%Si (mass fraction, the same in the following) master alloy, commercial pure aluminum (99.8%) and pure Fe (99.9%). The materials were melted in a resistance furnace at 850 °C and the melt was degassed for 10 min with argon gas through a graphite lance. The melt was cooled down to a temperature of 750−780 °C after degassing. The metal cup was preheated to 530−550 °C by the heating furnace. Subsequently, about 400 g liquid metal was poured into the preheated metal cup. The USV was then applied on the melt with the ultrasonic vibrator immersing into the melt 15−20 mm in depth when the liquid metal cooled down to the predetermined temperature. After the melt was treated with USV for a certain time, the semi-solid slurry with a certain solid fraction was obtained. In order to study the microstructure of the slurry after USV treatment, some slurry was extracted out by a quartz tube with an inner diameter of 6 mm and quenched in water immediately to get quenched rods. For comparison, some of the melt without USV treatment was cooled to the same temperature with the same cooling rate and then quenched in water immediately. The remaining slurry treated by USV was then poured into a cast iron mold preheated at 200 °C to get samples with diameter of 10 mm. For comparison, conventional casting samples formed at the temperature of 750 °C were also produced without USV treatment.

The JMat Pro software was used to calculate the start-freezing temperature of primary Si and primary Fe-containing intermetallic compounds in the Al−17Si−xFe alloys. The calculated results presented in Table 1 were used as the reference of the starting and ending temperatures of the USV treatment. The temperature range of USV treatment was 20 °C and the treatment time was 1.5−2.0 min. Table 2 presents the parameters of the USV treatment for Al−17Si−xFe alloys.

Table 1 Start-freezing temperature of primary crystals of Al−17Si−xFe alloys calculated by JMat Pro software

Alloy	Start-freezing temperature/°C	
	Primary Si	Primary Fe-containing intermetallic compounds
Al−17Si−2Fe	640	619
Al−17Si−3Fe	638	640
Al−17Si−4Fe	640	661
Al−17Si−5Fe	642	679

Table 2 Parameters of USV treatment for Al−17Si−xFe alloys

Alloy	Starting temperature/°C	Ending temperature/°C	Treatment time/min
Al−17Si−2Fe	650	630	2.0
Al−17Si−3Fe	655	635	1.6
Al−17Si−4Fe	675	655	1.9
Al−17Si−5Fe	697	677	1.7

Specimens for the metallographic examination were cut from the samples and the quenched rods, then ground, polished and etched by solution with 5% sodium hydroxide. The microstructures were examined using an Axiovert 200MAT optical microscope. Micrographs of the specimens were analyzed using a quantitative metallographic analysis software. Phase constitution and composition of different phases were studied by Quanta 200 environmental scanning electron microscope (SEM) fitted with an energy dispersive X-ray spectroscopy (EDX). X-ray diffraction (XRD) analysis was carried out with an X'Pert PRO diffractometer.

3 Results

3.1 Microstructures of Al−17Si−*x*Fe alloys produced by conventional casting process

Figure 1 shows the as-cast microstructures of Al−17Si−*x*Fe alloys produced by conventional casting process. The microstructures of Al−17Si−*x*Fe alloys all consist of polygonal primary Si, long needle-like phase, plate-like or coarse needle-like phase and eutectic structure. With the increase of Fe content from 2% to 5% in the Al−17Si−*x*Fe alloys, the amount of plate-like or coarse needle-like phase increases while the amount of long needle-like phase decreases. XRD analysis shows that Al−17Si−*x*Fe alloys all contain β-Al_5FeSi phase and δ-Al_4FeSi_2 phase. EDX analysis indicates that Al, Si and Fe elements are observed in the long needle-like compound, the plate-like compound and the coarse needle-like compound of Al−17Si−*x*Fe alloys, as illustrated in Table 3. It is clear that the plate-like compound and coarse needle-like compound are close to δ-Al_4FeSi_2 and the long needle-like compound is close to β-Al_5FeSi based on the compositions of the compounds. The δ-Al_4FeSi_2 phase is often present in high-silicon alloys and it has platelet morphology, whereas the β-Al_5FeSi phase has a distinctive needle morphology [4]. The needle-like β-Al_5FeSi phase coexists with plate-like δ-Al_4FeSi_2 phase in as-cast Al−20Si−2.0Fe−2.0Cu−0.4Mg−1.0Ni alloy produced by conventional casting process [6]. The Fe-containing intermetallic compounds are mainly composed of coarse needle-like δ-Al_4FeSi_2 phase in as-cast Al−25Si−5Fe−3Cu alloy [7] and Al−25Si−5Fe alloy [16]. It can therefore be concluded that the plate-like or coarse needle-like compound should be δ-Al_4FeSi_2 phase and the long needle-like compound should be β-Al_5FeSi in Al−17Si−*x*Fe alloys, as shown in Fig. 1.

To sum up, with the increase of Fe content from 2% to 5% in Al−17Si−*x*Fe alloys produced by conventional casting process, the amount of plate-like or coarse needle-like δ-Al_4FeSi_2 phase increases while the amount of long needle-like β-Al_5FeSi phase decreases.

3.2 Microstructures of Al−17Si−*x*Fe alloys with USV treatment

Figure 2 shows the as-cast microstructures of Al−17Si−*x*Fe alloys with USV treatment. The microstructures of Al−17Si−*x*Fe alloys all consist of polygonal primary Si, a large amount of block compounds, a small amount of β-Al_5FeSi phase and eutectic structure. The XRD analysis shows that

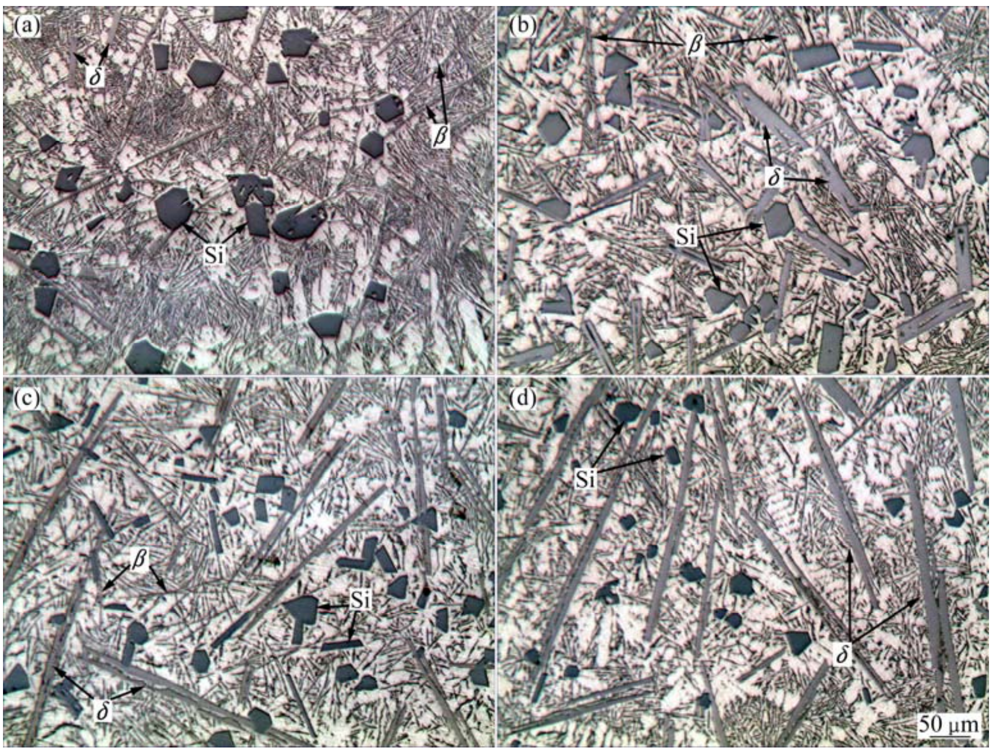

Fig. 1 Microstructures of Al−17Si−*x*Fe alloys produced by conventional casting process: (a) Al−17Si−2Fe; (b) Al−17Si−3Fe; (c) Al−17Si−4Fe; (d) Al−17Si−5Fe

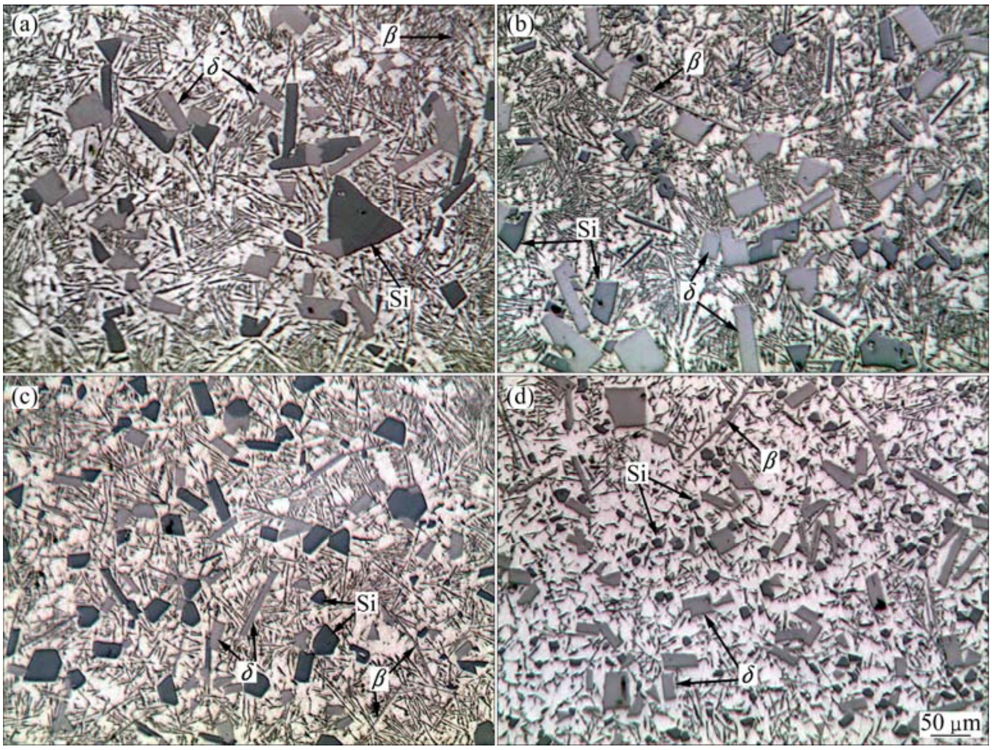

Fig. 2 Microstructures of Al−17Si−xFe alloys with USV treatment: (a) Al−17Si−2Fe; (b) Al−17Si−3Fe; (c) Al−17Si−4Fe; (d) Al−17Si−5Fe

Table 3 EDX results of intermetallic compounds in Al−17Si−xFe alloys produced with conventional casting process

Alloy	Phase	Mole fraction, %		
		Al	Si	Fe
Al−17Si−2Fe	Long needle-like intermetallic compound	66.86	18.41	14.73
Al−17Si−2Fe	Plate-like intermetallic compound	50.04	32.01	17.94
Al−17Si−5Fe	Coarse needle-like intermetallic compound	49.81	32.71	17.48

Al−17Si−xFe alloys with USV treatment all contain δ-Al_4FeSi_2 phase and β-Al_5FeSi phase, as shown in Fig. 3. EDX analysis indicates that the block compounds of Al−17Si−xFe alloys contain the same elements of Al, Si and Fe, as shown in Table 4. It is clear that the block compounds are close to δ-Al_4FeSi_2 based on the compositions. Thus, the block compounds in Fig. 2 should be δ-Al_4FeSi_2. In other words, the morphology of the Fe-containing intermetallic compounds in Al−17Si−xFe alloys is changed by USV, but the phase constitutions of these alloys keep invariant.

Based on the metallographic analysis software, the average grain size of δ-Al_4FeSi_2 particles of Al−17Si−2Fe, Al−17Si−3Fe, Al−17Si−4Fe and Al−17Si−5Fe alloys with USV treatment are 31, 37, 26 and 29 μm respectively. Compared with the Fe-containing intermetallic compounds with a length of 100−200 μm in Fig. 1, the compounds in Fig. 2 are obviously refined.

4 Discussion

Two phenomena exist when ultrasound propagates in the melt, i.e, acoustic streaming and cavitation. The occurrence of cavitation bubbles in the melt can increase the heterogeneous nucleation of crystallization. This can be further explained by three mechanisms. First of all, during the growth and rapid expansion of the bubbles, the liquid evaporates inside the bubble and the evaporation process reduces the temperature of bubbles. A decrease in the bubble temperature below the equilibrium temperature results in melt undercooling at the bubble surface, hence a nucleus will form on a bubble [17]. Secondly, the energy of collapsing cavitation bubbles is transformed into pressure pulses up to 1000 MPa and cumulative jets up to 100 m/s [18]. According to the Clapeyron equation, the pressure pulse arising from the collapsing of bubbles alters the melting point (T_m). An increase in T_m is equivalent to the increase of undercooling, so that an enhanced nucleation event is expected [19]. Thirdly, non-metallic compounds and oxide particles that pre-exist in the melt or are formed during solidification are not wetted by the melt. Because the defects (cavities, cracks and recesses) on the surfaces

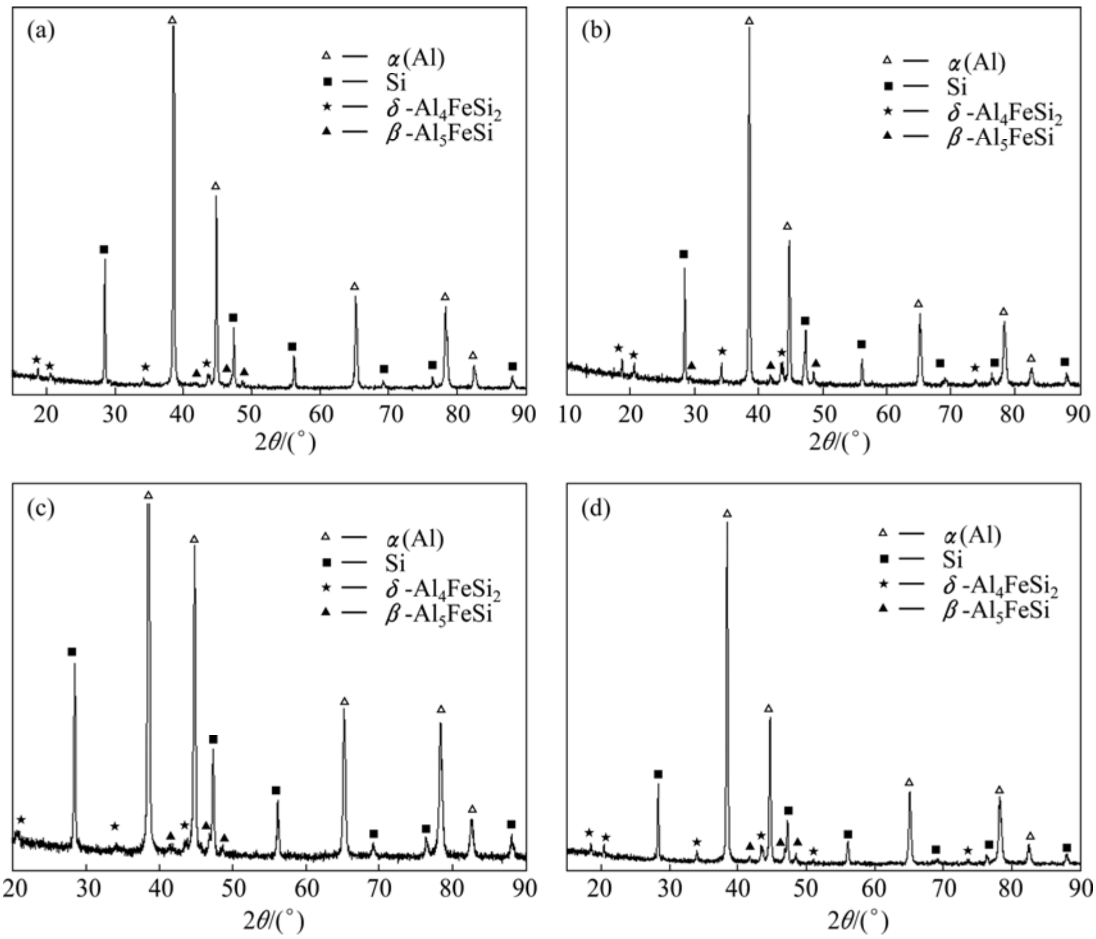

Fig. 3 XRD patterns of Al−17Si−xFe alloys with USV treatment: (a) Al−17Si−2Fe; (b) Al−17Si−3Fe; (c) Al−17Si−4Fe; (d) Al−17Si−5Fe

Table 4 EDX results of block intermetallic compounds in Fig. 2

Alloy	Composition (mole fraction)/%		
	Al	Si	Fe
Al−17Si−2Fe	50.10	32.60	17.30
Al−17Si−3Fe	49.60	32.61	17.79
Al−17Si−4Fe	50.20	31.43	18.37
Al−17Si−5Fe	51.76	31.17	16.88

are filled with gaseous phase, these particles could not become the substrates for heterogeneous nucleation. The high pressure pulses and cumulative jets, which are produced by the collapsing of cavitation bubbles, lead to the wetting of the impurities with molten metal. Consequently, this enables the inert impurities to act as solidification nuclei [20].

Figure 4(a) shows the microstructure of semi-solid slurry of Al−17Si−2Fe alloy without USV treatment quenched at 630 °C. The microstructure consists of polygonal primary Si with dark grey color, a small amount of α(Al) dendrites and fine ternary eutectic structure formed during rapid water-cooling. XRD analysis (Fig. 5(a)) indicates that the slurry shown in Fig. 4(a) contains α(Al), Si and β-Al_5FeSi phase. It is clear that only primary Si phase precipitates before quenching at 630 °C. Thus, the equilibrium solidification of Al−17Si−2Fe alloy starts with the formation of primary Si phase. Figure 4(b) shows the microstructure of semi-solid slurry of Al−17Si−2Fe alloy treated by USV from 650 °C to 630 °C. The microstructure is composed of polygonal primary Si, block δ-Al_4FeSi_2 phase, a small amount of α(Al) dendrites and fine ternary eutectic structure formed during rapid water-cooling. XRD analysis (Fig. 5(b)) indicates that the slurry shown in Fig. 4(b) contains α(Al), Si, δ-Al_4FeSi_2 and β-Al_5FeSi phases. By comparing Fig. 4(a) with Fig. 4(b), it can therefore be concluded that cavitation increases the start-freezing temperature of δ-Al_4FeSi_2 phase during the USV treatment of Al−17Si−2Fe alloy, and δ-Al_4FeSi_2 phase also precipitates before quenching at 630 °C. In other words, the temperature range of nucleation and growth for δ-Al_4FeSi_2 phase grains are enlarged. The phenomenon that cavitation can increase the start-

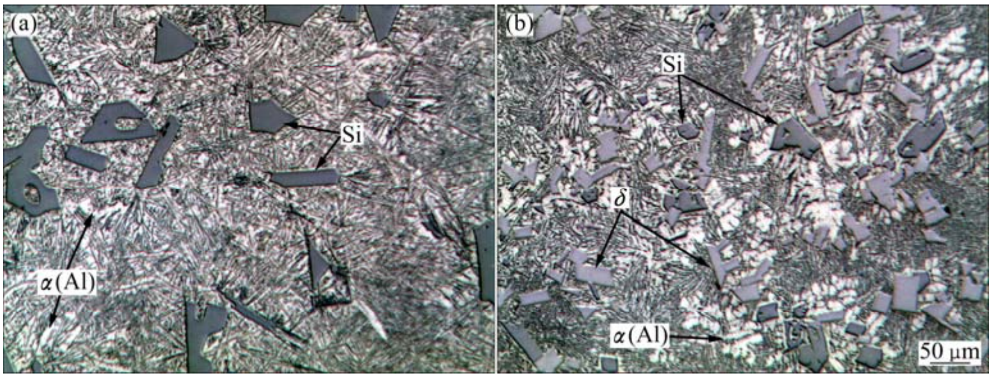

Fig. 4 Microstructures of semi-solid slurry of Al−17Si−2Fe alloy quenched at 630 °C: (a) Without USV treatment; (b) With USV treatment

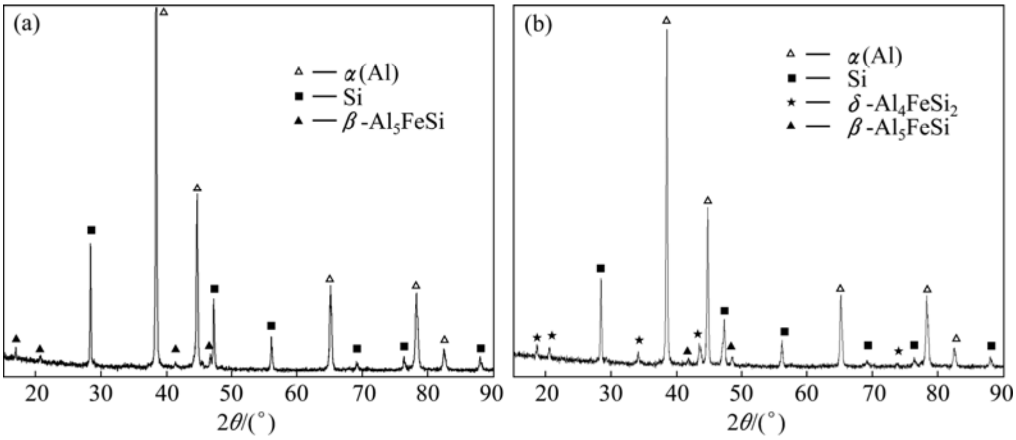

Fig. 5 XRD patterns of semi-solid slurry of Al−17Si−2Fe alloy quenched at 630 °C: (a) Without USV treatment; (b) With USV treatment

freezing temperature of δ-Al_4FeSi_2 phase has not been reported in existing literatures.

Furthermore, according to the ternary phase diagram [21], the equilibrium solidification of Al−17Si−(3, 4, 5)Fe alloys with the Fe content equal or more than 3%, starts with the formation of δ-Al_4FeSi_2 phase, followed by the formation of the primary Si phase. Thus, when the melt of Al−17Si−xFe alloys is treated by USV near the liquidus temperatures (Table 2) for a certain time, the temperature range of nucleation and growth for δ-Al_4FeSi_2 phase grains is increased by cavitation.

As can be seen from Fig. 1, δ-Al_4FeSi_2 phase is plate-like or coarse needle-like and its length-to-width ratio is large and increases with increasing Fe content. This is mainly due to the significantly different solid-liquid (S-L) interfacial energy at the solidifying front along different directions. Consequently, the disparities in growth rates along different crystallographic directions are great. In contrast, as shown in Fig. 2, the δ-Al_4FeSi_2 phase is modified into block or short plate-like phase after USV treatment and its length-to-width ratio is much smaller than that in Fig. 1. This is mainly because of the acoustic streaming. In the binary Al−Fe system, the equilibrium solid solubility of Fe in Al is in the range of 0.03%−0.05% at the eutectic temperature of 655 °C and less than 0.01% at 427 °C [22]. Consequently, Fe segregates during solidification and tends to combine with Al and other elements to form intermetallic compounds of various types. The speed of acoustic streaming produced by USV is 5−10 times of heat convection speed in the melt [23]. The acoustic streaming plays a very important role in homogenizing the solute field and the temperature field of the melt, accelerating the heat and mass transfer, reducing the thickness of diffusion layer at the S-L interface as well as dispersing the primary nuclei. This is expected to lower the compositional difference at the S-L interface and reduce the differences in S-L interfacial energies, which will slow down the preferential growth of δ-Al_4FeSi_2 phase in the longitudinal direction. As a result, the length-to-width ratio of δ-Al_4FeSi_2 phase decreases after USV treatment. Figure 6 shows the three-dimensional morphology of Al−17Si−4Fe alloy with USV treatment observed by SEM on the deep-

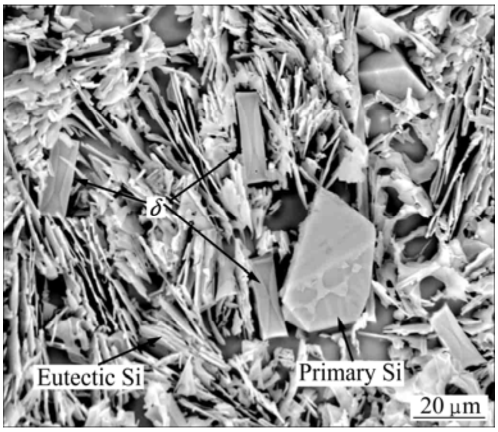

Fig. 6 SEM micrograph of deep-etched sample of Al−17Si−4Fe alloy with USV treatment

etched samples. It can be seen that δ-Al_4FeSi_2 phase grains are changed into small blocks by USV.

A large amount of crystal nuclei of δ-Al_4FeSi_2 phase formed due to cavitation are dispersed uniformly into the melt by intensive convection induced by acoustic streaming. During the growth stage, the preferential growth of δ-Al_4FeSi_2 phase along longitudinal direction is weakened. These could explain the morphological changes of δ-Al_4FeSi_2 phase from plate-like or coarse needle-like to block or short plate-like in Al−17Si−xFe alloys.

Besides, the reason that a small amount of β-Al_5FeSi phases remain in the matrix of Al−17Si−xFe alloys with USV treatment is as follows. According to the Al−Si−Fe ternary phase diagram [21], in the equilibrium solidification process of Al−17Si−xFe alloys, the previously formed δ-Al_4FeSi_2 phase transforms into β-Al_5FeSi phase with peritectic reaction L+δ-Al_4FeSi_2→ β-Al_5FeSi+Si at the temperature below 600 °C. After that, at about 576 °C, the ternary eutectic structure consisting of α(Al), Si phase and β phase is formed.

In particular, for Al−17Si−2Fe alloy, the temperature range from the start-freezing temperature of δ-Al_4FeSi_2 phase to 600 °C, is the narrowest in the Al−17Si−xFe alloys produced by conventional casting process. This is also the main reason why the Fe-containing intermetallic compounds exist mainly as long needle-like β-Al_5FeSi phase in Al−17Si−2Fe alloy, as shown in Fig. 1(a). When the melt is treated by USV, large undercooling caused by cavitation not only promotes the formation of nuclei of δ-Al_4FeSi_2 phase but also enlarges the temperature range of crystallization and growth for δ-Al_4FeSi_2 phase. Therefore, the amount of needle-like β-Al_5FeSi phase decreases greatly in Al−17Si−2Fe alloys after USV treatment.

5 Conclusions

1) The Fe-containing intermetallic compounds are mainly composed of long needle-like β-Al_5FeSi phase with a small amount of plate-like δ-Al_4FeSi_2 phase in Al−17Si−2Fe alloy produced by conventional casting process. With the increase of Fe content from 2% to 5% in the Al−17Si−xFe alloys, the amount of plate-like or coarse needle-like δ-Al_4FeSi_2 phase increases while the amount of long needle-like β-Al_5FeSi phase decreases.

2) The size and morphology of Fe-containing intermetallic compounds in Al−17Si−xFe alloys are refined after USV treatment for 1.5−2.0 min. They mainly exist as particle-like δ-Al_4FeSi_2 phase with grain size ranging from 26 μm to 37 μm, and only a small amount of β-Al_5FeSi phases remain.

3) The effect of USV leads to the formation and refinement of δ-Al_4FeSi_2 phase. Acoustic streaming and cavitation of USV homogenize the solute field and temperature field, and increase the start-freezing temperature of δ-Al_4FeSi_2 phase, thereby promoting the formation of fine δ-Al_4FeSi_2 particles.

References

[1] KAPRANOS P, KIRKWOOD D H, ATKINSON H V, RHEINLANDER J T, BENTZEN J J, TOFT P T, DEBEL C P, LASLAZ G, MAENNER L, BLAIS S, RODRIGUEZ-IBABE J M, LASA L, GIORDANO P, CHIARMETTA G, GIESE A. Thixoforming of an automotive part in A390 hypereutectic Al−Si alloy [J]. Journal of Materials Processing Technology, 2003, 135: 271−277.

[2] WU Shu-sen, TU Xiao-lin, FUKUDA Y, KANNO T, NAKAE H. Modification mechanism of hypereutectic Al−Si alloy with P−Na addition [J]. Transactions of Nonferrous Metals Society of China, 2003, 13: 1285−1289.

[3] COUTURE A. Iron in aluminium casting alloys—A literature survey [J]. AFS International Cast Metals Journal, 1981, 6(4): 9−17.

[4] MBUYA T O, ODERA B O, NG'ANG'A S P. Influence of iron on castability and properties of aluminium silicon alloys: Literature review [J]. International Journal of Cast Metals Research, 2003, 16(5): 451−465.

[5] TAYLOR J A, SCHAFFER G B, STJOHN D H. The role of iron in the formation of porosity in Al−Si−Cu-based casting alloys: Part II. A phase-diagram approach [J]. Metallurgical and Materials Transactions A, 1999, 30(6): 1651−1655.

[6] ZHONG Gu, WU Shu-sen, JIANG Hua-wen, AN Ping. Effects of ultrasonic vibration on the iron-containing intermetallic compounds of high silicon aluminum alloy with 2% Fe [J]. Journal of Alloys and Compounds, 2010, 492: 482−487.

[7] HOU L G, CUI H, CAI Y H, ZHANG J S. Effect of (Mn+Cr) addition on the microstructure and thermal stability of spray-formed hypereutectic Al−Si alloys [J]. Materials Science and Engineering A, 2009, 527: 85−92.

[8] AHMAD R, MARSHALL R I. Effect of superheating on iron-rich plate-type compounds in aluminium-silicon alloys [J]. International Journal of Cast Metals Research, 2003, 15: 497−504.

[9] SRIVASTAVA A K, SRIVASTAVA V C, GLOTER A, OJHA S N.

Microstructural features induced by spray processing and hot extrusion of an Al−18%Si−5%Fe−1.5%Cu alloy [J]. Acta Materialia, 2006, 54: 1741−1748.

[10] BELOV N A, ESKIN D G, AKSENOV A A. Multicomponent phase diagrams: Applications for commercial aluminum alloys [M]. Oxford: Elsevier, 2005: 43.

[11] ZHAO Jun-wen, WU Shu-sen, WAN Li, CHEN Qi-hua, AN Ping. Evolution of microstructure of semisolid metal slurry in ultrasound field [J]. Acta Metallurgica Sinica, 2009, 45(3): 314−319. (in Chinese)

[12] WU Shu-sen, ZHONG Gu, WAN Li, AN Ping, MAO You-wu. Microstructure and properties of rheo-diecast Al−20Si−2Cu−1Ni−0.4Mg alloy with direct ultrasonic vibration process [J]. Transactions of Nonferrous Metals Society of China, 2010, 20(3): s763−s767.

[13] ZHAO Jun-wen, WU Shu-sen, AN Ping, MAO You-wu. Preparation of semi-solid slurry of hypereutectic Al−Si alloy by ultrasonic vibration [J]. Solid State Phenomena, 2008, 141−143: 767−771.

[14] OSAWA Y, TAKAMORI S, KIMURA T, MINAGAWA K, KAKISAWA H. Morphology of intermetallic compounds in Al−Si−Fe alloy and its control by ultrasonic vibration [J]. Materials Transactions, 2007, 48(9): 2467−2475.

[15] KHALIFA W, TSUNEKAWA Y, OKUMIYA M. Effect of ultrasonic treatment on the Fe-intermetallic phases in ADC12 die cast alloy [J]. Journal of Materials Processing Technology, 2010, 210: 2178−2187.

[16] HUANG H J, CAI Y H, CUI H, HUANG J F, HE J P, ZHANG J S. Influence of Mn addition on microstructure and phase formation of spray-deposited Al−25Si−*x*Fe−*y*Mn alloy [J]. Materials Science and Engineering A, 2009, 502: 118−125.

[17] ABRAMOV V O, ABRAMOV O V, STRAUMAL B B, GUST W. Hypereutectic Al−Si based alloys with a thixotropic microstructure produced by ultrasonic treatment [J]. Materials & Design, 1997, 18(4−6): 323−326.

[18] ESKIN G I. Broad prospects for commercial application of the ultrasonic (cavitation) melt treatment of light alloys [J]. Ultrasonics Sonochemistry, 2001, 8(3): 319−325.

[19] QIAN M, RAMIREZ A, DAS A. Ultrasonic refinement of magnesium by cavitation: Clarifying the role of wall crystals [J]. Journal of Crystal Growth , 2009, 311(14): 3708−3715.

[20] ESKIN G I, MAKAROV G S, PIMENOV YU P. Effect of ultrasonic processing of molten metal on structure formation and improvement of properties of high-strength Al−Zn−Mg−Cu−Zr alloys [J]. Advanced Performance Materials, 1995, 2: 43−50.

[21] PETZOW G, EFFENBERG G. Ternary alloys: A comprehensive compendium of evaluated constitutional data and phase diagrams [M]. Vol.3. Weinheim, Germany: VCH, 1988: 404−421.

[22] MONDOLFO L F. Aluminum alloys: Structure and properties [M]. London: Butterworths, 1976: 283−284.

[23] WU Shu-sen, ZHAO Jun-wen, ZHANG Li-ping, AN Ping, MAO You-wu. Development of non-dendritic microstructure of aluminum alloy in semi-solid state under ultrasonic vibration [J]. Solid State Phenomena, 2008, 141−143: 451−456.

超声振动对高铁含量过共晶铝硅合金中富铁相的影响

林 冲，吴树森，钟 鼓，万 里，安 萍

华中科技大学 材料成形与模具技术国家重点实验室，武汉 430074

摘 要：铝硅合金中的高熔点富铁相可以提高合金的热稳定性及耐磨性，但传统铸造工艺下富铁相的长针状形态对基体强度有不利影响。研究超声处理对不同铁含量过共晶 Al−17Si−*x*Fe(*x*=2，3，4，5)合金中富铁相形态变化的影响。结果表明，在传统铸造工艺下，含铁量为 2%的铸态合金组织中的富铁相主要由长针状 β-Al_5FeSi 相以及少量片状 δ-Al_4FeSi_2 相组成。随着铁含量从 2%增加到 5%，合金组织中长针状 β-Al_5FeSi 相逐渐减少，片状或粗大针片状 δ-Al_4FeSi_2 相逐渐增多。含铁量为 5%时，合金组织以粗大针片状 δ-Al_4FeSi_2 相为主。经超声处理后，合金中富铁相被细化，主要以块状 δ-Al_4FeSi_2 相形式存在，并含有少量针状 β-Al_5FeSi 相；δ 相的平均晶粒尺寸在 26~37 μm 之间，明显细化。初步探讨了超声处理对富铁相形态变化的作用机理。

关键词：过共晶铝硅合金；超声振动；富铁相

(Edited by Sai-qian YUAN)